Colloids and Surfaces A: Physicochem. Eng. Aspects 413 (2012) 50–57

Contents lists available at SciVerse ScienceDirect

Colloids and Surfaces A: Physicochemical and Engineering Aspects

journal homepage: www.elsevier.com/locate/colsurfa

Characterization of porous media by dynamic wicking combined with image analysis

Eleni Fragiadaki[a,1], Stefanos Harhalakis[a,1], Eleni P. Kalogianni[b,*]

[a] Department of Informatics, Alexander Technological Educational Institution of Thessaloniki, P.O. Box 141, 57400 Thessaloniki, Greece
[b] Department of Food Technology, Alexander Technological Educational Institution of Thessaloniki, P.O. Box 141, 57400 Thessaloniki, Greece

ARTICLE INFO

Article history:
Received 30 October 2011
Received in revised form 19 February 2012
Accepted 20 February 2012
Available online 28 February 2012

Keywords:
Dynamic wicking
Image analysis
Porous media

ABSTRACT

Dynamic wicking is a well-known technique for the determination of contact angles between porous media (or powders) and liquids, the determination of surface properties and pore sizes. Wicking data have the form of weight or optical measurements. Acquiring and analysing weight data is easy and appropriate instruments can be found in the market. On the other hand, optical data carry a lot of information that cannot be retrieved by weight measurements. The optical observation of the wicking phenomenon can reveal heterogeneities in the material under investigation related to its pore structure and/or surface properties. This information can be of significant technological importance for several applications such as yarns and textiles, porous food systems, and powders. Unfortunately, to our knowledge, no commercial instrument providing analysis of optical data of dynamic wicking exists.

The aim of this work was to develop an algorithm, program and user-friendly software for the analysis of dynamic wicking images and explore its capabilities. The application refers to wicking experiments where the wicking front propagates towards one direction. In order to cover a wide range of possible cases we performed numerous wicking experiments. In the experiments, porous materials having different properties (surface roughness, pore sizes and pore size distribution, transparency, ability to reflect light) were used. In addition, during the wicking tests we caused several lighting disturbances (uneven lighting, lighting that changes over time, etc.) aiming to best simulate actual experimental conditions and further stress the capabilities of the algorithm. Results of the developed application are compared with results analysed without it. Finally, we performed wicking tests on two biological materials and local analysis of the wicking data was applied. The technological significance of these results is discussed. The program can provide global and local information of the wicking phenomenon giving as an output the distance vs time data. These data can be used for the determination of contact angles, surface properties and effective mean pore radii of the material. The application can be used as stand-alone as well as a module of already existing axisymmetric drop shape analysis instruments.

1. Introduction

Dynamic wicking is a well-known technique for the determination of contact angles between porous media (or powders) and liquids, the determination of surface properties and pore sizes in both inorganic and biological porous material [1–4]. The technique is based on describing the kinetics of spontaneous liquid penetration due to capillary forces inside a thin layer of material (powder or porous medium) by the Lukas–Washburn equation [5]. There are two main experimental set-ups for wicking experiments. In the first case, this is the commonest amongst researchers, the wicking front advances towards one direction (vertically or horizontally) [1,3]. This type of experiment gives an approximately linear wicking front. Some researchers (mainly those working with textiles) perform a different type of experiment where the wicking liquid is fed in the centre of a (horizontally positioned) material. In this case the liquid penetrates the material forming a circle-like wicking front [6,7]. In vertical wicking and depending on the system characteristics (porous medium height and pore sizes, liquid/solid contact angle, liquid surface tension and density) the wicking rate may be significantly affected by gravity and therefore the Lukas–Washburn equation cannot adequately describe liquid penetration. This is not a limitation to vertical wicking because one can take gravity effects into account [8].

This work deals with wicking experiments where the wicking front advances towards one direction (vertical or horizontal). In these types of experiments monitoring the wicking phenomenon

* Corresponding author. Tel.: +30 2310 013907; fax: +30 2310 791369.
E-mail addresses: eleni.fra@gmail.com (E. Fragiadaki), v13@acm.org (S. Harhalakis), elekalo@food.teithe.gr (E.P. Kalogianni).
[1] Present address: Department of Applied Informatics, University of Macedonia Economic and Social Sciences, 54006 Thessaloniki, Greece.

0927-7757/$ – see front matter © 2012 Elsevier B.V. All rights reserved.
doi:10.1016/j.colsurfa.2012.02.031

can be performed either by measuring the distance the liquid front advances into a porous medium or the increase in the mass of the solid induced by filling its pores. The analysis of both types of data can be considered equivalent provided that (a) the appropriate values of porosity are used to convert weight into height data and (b) the weight of the meniscus forming at the surface of the porous medium simultaneously with capillary penetration is taken into account when weight data are considered [9]. Due to those two considerations the analysis of weight data is more complicated than the one for optical data. Nevertheless, acquiring weight data is easy and probably this is why the weight measurement principle is recently used more often for wicking experiments. Moreover, instruments found in the market are based on the weight measurement principle.

On the other hand, optical data provide more straight forward information (i.e. no corrections have to be made) but what is more important optical data can reveal heterogeneities of the material under investigation related to its pore structure and/or its surface properties. These heterogeneities are observed as variations of the height of the wicking front along the material. However, when performing weight measurements these variations are averaged and therefore information on heterogeneity is lost. The observed variations in the wicking behaviour within the same measurement can reveal not only a variation in pore sizes (variations in pore sizes can be also determined using other techniques) but also changes in pore interconnectivity (e.g. blocked pores) and variations in the tortuosity of the pore structure (information difficult to obtain by other means). Furthermore, they can reveal variations in the material surface properties which can be essential for composite materials. Variations in pore sizes/tortuosity can be distinguished from variations in the porous material surface properties by performing wicking experiments in the same material with both unpolar and polar liquids [1]. Measurements of the variation of wicking behaviour have also a technological importance as they show how the material performs under actual imbibition conditions with several applications such as yarns and textiles, porous food systems, and powders. Fluctuations on the wicking front have been observed and qualitatively discussed in biological materials [3,10] however they have not been quantitatively exploited in the past to the best of our knowledge.

The automation of analysis of wicking images has first been attempted in 1990 [11]. Nevertheless, there exists no commercial instrument in the market providing analysis of optical dynamic wicking data to the best of our knowledge. This is probably due to the fact that although the acquisition of optical data has become easy with the fast cameras and powerful computers the analysis of these data to determine with accuracy the wicking front is not trivial. Powders but mainly porous material such as porous foods, textiles and filters have a rough surface and several black spots appear on the image. These spots can be often of the same or similar grey-scale level (or colour) as the wetted material. This, as a consequence, often confuses the algorithms used for the analysis of wicking images. So although lately some researchers have made attempts to analyse such images using different algorithms [6,7] results are not always satisfactory, no such commercial application exists and even nowadays many researchers analyse wicking data manually [9,10] even though this is an extremely time-consuming procedure.

In this work we develop an algorithm, program and user-friendly software for the analysis of dynamic wicking images and test its performance. The software provides global as well as local information on the wicking behaviour. Its final goal is to give average values on the desired properties of the examined material and describe material heterogeneity with local values wherever needed. In addition to developing the program, we performed numerous wicking experiments in order to cover a wide range of possible experimental cases. In the experiments porous materials having different properties (surface roughness, pore sizes and pore size distribution, transparency, ability to reflect light) were used. Moreover, during the wicking tests we caused several lighting disturbances (uneven lighting, lighting that changes over time, etc.) aiming to best simulate actual experimental conditions and further stress the capabilities of the algorithm. We also performed a series of tests where results of the developed application were compared with those obtained by a "manual" analysis of the images. Finally, we analyse optical wicking data of two biological materials with heterogeneous porous structure and discuss the technological significance of the results.

2. Development of the program

The aim of the program is to automate the determination of the position of the wicking front in dynamic wicking experiments where the wicking front propagates towards one direction. First, the determination of an average wicking front line is addressed whereas local properties are addressed below. The input data for the program is a number of consecutive images depicting the progression of the wicking phenomenon over time. The program aims at the creation of a number of photographs where a line will be drawn on the position of the wicking front, in addition to a number of values (wicking height in pixels and actual size and time values corresponding to each image in the experiment) based on the measurements.

In order to design and implement the specific program the following factors that affect the outcome of the measurements have to be considered:

1. An experiment consists of more than one images.
2. The images may be in grey-scale or colour.
3. The experiment evolves over time.
4. Different materials are immersed in the liquid and each one of them has different characteristics like colour and surface anomalies. These characteristics affect the way the material is depicted in the captured image as spots or lines of darker colour appear in several areas of the material. In some cases these spots or lines are of even darker colour than the areas filled with liquid. These differences can create the impression that parts of the material have been filled with liquid whereas that might not be true.
5. The liquid does not rise (or penetrate) uniformly. Several fluctuations appear since there are areas in the photographs where the liquid rises more in comparison with other neighbouring areas.
6. Very often recorded images present notable changes in the luminosity in both the horizontal and the vertical axes. Furthermore notable changes in the luminosity amongst images of the same wicking experiment may appear.

Originally, we examined a number of edge detection methods that include algorithms for detecting the edges of objects present in a photograph. Such algorithms are the Sobel algorithm, the Laplace, the Prewitt compass method, the Roberts method and the Differential edge detection method. In general, edge detection algorithms are based on applying a mask to the original image. This mask transforms the original image either to a new one, at which the edges are highlighted, or to an intermediate image, at which another mask is applied. In the resulting image the edges are highlighted in order for us to clearly distinguish them from the background.

For the solution of the specific problem these algorithms/methods were tested with minimum adjustments, without trying to fine-tune them. The tests indicated that even though in some cases the methods came close in identifying the desired front-line they were not capable of specifically defying it. In

addition, these algorithms cannot distinguish amongst pixels with different colours, which do not imply an edge but a difference in the luminosity, surface roughness or a distortion of the material used. Moreover even if the above methods were able to exactly, or with a good approximation detect the wicking front, we would have to programmatically detect the position of the front at a later time since the algorithms produce an image with highlighted edges and not the positions of the pixels that consist the line (wicking front). Consequently, we decided to create an algorithm that would initially detect the proper position of the wicking front. After that, the algorithm should be modified to consider all the photographs of the experiment and all the factors mentioned above, such as the changes in luminosity in the same or in consecutive photographs, the fluctuations in the wicking height in different areas of the material, etc.

The collection of images, accompanied with the times at which each image was acquired is considered as input to the algorithm. The times are needed in order to identify the ordering of the images and provide distance vs time output later on. During the processing of an image we assume that the liquid can only further penetrate in the porous medium, thus the height at which the liquid has risen (or distance has penetrated) can be either greater or equal to the distance the liquid had reached at the previous image.

The algorithm processes an image starting either at the bottom or from a predefined position and moving upwards. Its main purpose is to examine the individual pixels of the grey-scaled photograph and to transform them into black or white (depending on whether they have been covered in liquid or not). More specifically for each set of images comprising an experiment the program does the following:

1. The beginning of the wicking phenomenon (point 0) is manually defined. This point is not necessarily the same as the bottom of the image. Depending on how the image was acquired its lower part may include also the immersed part of the material under investigation the liquid bulk, etc. that should not be considered in the measurements.
2. The threshold is defined. The threshold controls the sensitivity of the algorithm in colour changes.

Then for each image in an experiment the algorithm:

1. Defines the starting point for the current image. The height of this point is set slightly beneath the wicking front identified in the previous photograph or to 0 if this is the first image. By doing so, the algorithm does not have to re-examine parts of the image that are already filled with the liquid as established by the analysis of the previous image. Also, the changes in colour should be considered in neighbouring areas since distant areas are more often affected by other factors, such as horizontal luminosity changes.
2. Transforms the image into grey-scale if it is in colour.
3. Applies the Blur and Auto Contrast methods to stretch the contrast and smoothen the photograph so that intense colour changes will not severely affect the processing of the photograph.
4. Applies an iterative procedure during which, starting beneath the point of the previously defined wicking front it separates the photograph into a number of equally sized vertical sections. This assists the algorithm in overcoming the vertical luminosity changes (if present). For each one of these sections, we consider the lower left pixel to be the starting point. Starting from that pixel, the algorithm examines whether its neighbouring pixels have been covered with liquid, and therefore the are transformed into black ("filled"), or not. If a pixel is filled then all neighbouring pixels are added to the list of pixels that should be examined next. The filling terminates either when the difference in colour of the current pixel and its neighbour is less than the fill threshold defined earlier, or when the difference in colour between the current pixel and the starting pixel is less than twice the fill threshold. After the filling has been terminated the algorithm picks the next pixel from the list and repeats the previous steps. If there are no more pixels in the list then the algorithm moves to the next section. After all sections have been examined the current iteration ends and the algorithm moves to the next iteration which starts beneath the maximum height calculated in the previous iteration. The iterations stop when the calculated wicking front for the specific photograph remains unchanged during two consecutive iterations.
5. The output of the algorithm is a new image, at which the line representing the position of the wicking front has been drawn, and for which the height in pixels has been calculated. It is important to note that there are cases where the liquid has penetrated further in some areas than in others that could result in different heights. The algorithm defines an average height based on the whole width of the image.

The programming language used was Python. For the graphical user interface (GUI) the Python Qt library was used and the Python PIL library was used for image manipulation operations.

The program facilitates the processing of the experiments and the definition of the following parameters:

1. the threshold of the experiment;
2. the point 0 (i.e. the position in the image where wicking begun) for all images in the experiment;
3. the parts of the photographs that we would not wish to include in the processing. These parts could refer to areas not covered with material (the material's width or height does not cover the width and/or height of the image) or could be considered invalid;
4. the calibration image that is going to be used as a reference scale for the transformation of pixels to actual dimensions;
5. the images that should be discarded. These images could be located at the beginning of the experiment (depicting the material as it is being immersed in the liquid or while calibrating the reading instrument) or at the end of the experiment (depicting a fully covered material at which point any further measurements are unnecessary).

Having defined these parameters the program processes the images of the experiment. Upon completion of the processing the program presents the newly created images where a line is drawn on the detected average position of the wicking front and a table of height (in pixels and actual distance) and time values corresponding to each image of an experiment. The images with the line can be used by the user in order to verify the accurate determination of the position of the line on the wicking front calculated by the program.

The height and time values can be exported to perform further calculations. In addition, the program produces a txt file with all parameters passed to the algorithm for future reference as long as a folder with the new photographs. The above steps can be seen schematically (Fig. 1).

When local information is required the procedure can be performed after dividing the material into areas. The areas are defined by the user according to the characteristics of each material. Then the analysis provides information on the user-defined areas.

A detailed description of the algorithm is given in Appendix A.

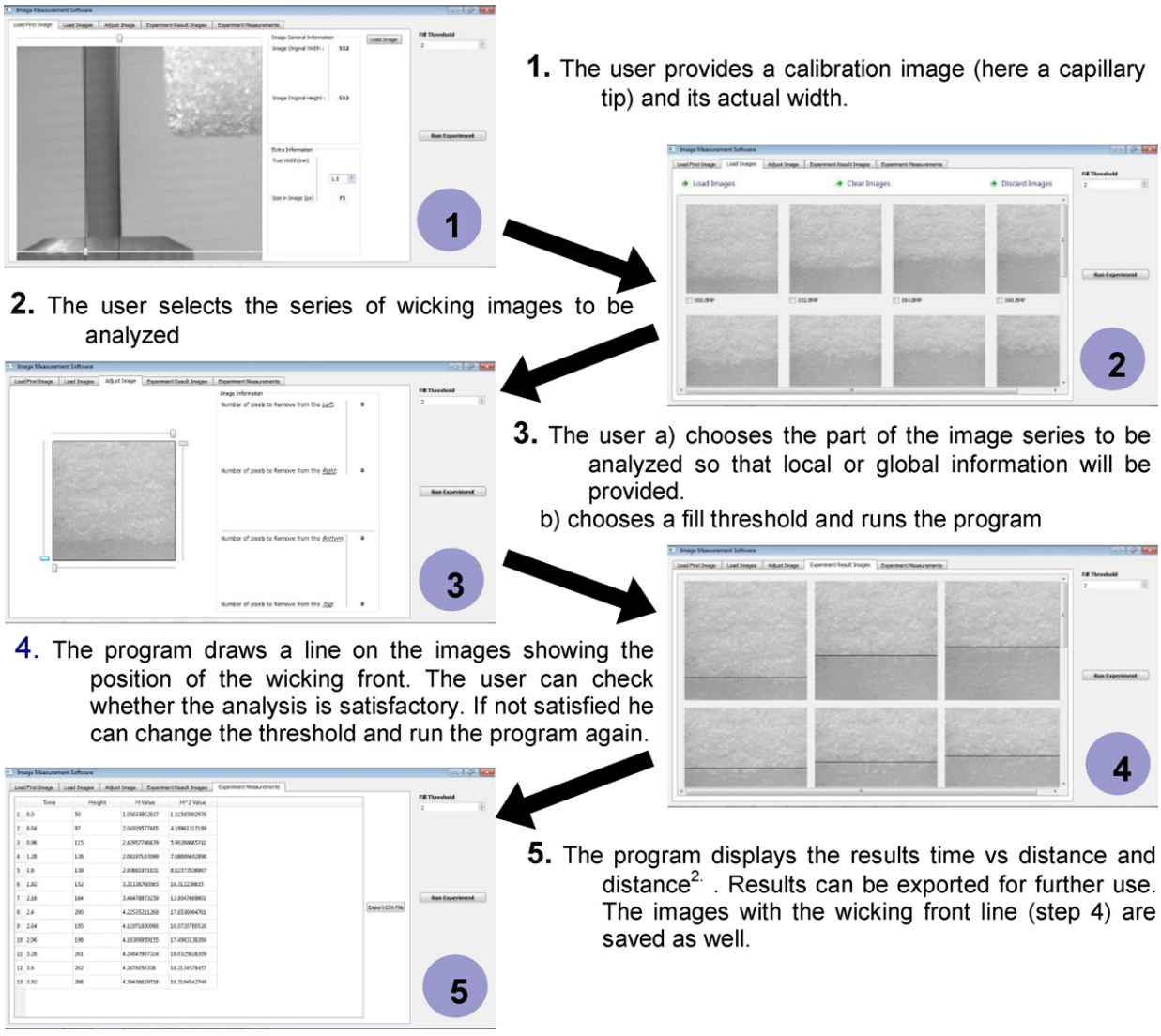

Fig. 1. Schematic representation of the steps followed for the analysis of optical wicking data.

3. Materials and methods

Different porous media were used for the experiments (Fig. 2). The porous media used and their characteristics are given below:

(a) Glass porous media (Robu, Germany): Lower surface roughness, small distribution of pore sizes, transparent and light reflecting. Pore sizes: 16–40 μm, 40–60 μm, 40–100 μm, 100–160 μm.
(b) Polymer porous media (Porex Technologies GmbH, Germany): Low surface roughness, small distribution of ore sizes, non-transparent, non-reflecting when dry but light reflecting when wet. Pore sizes: 7–12 μm, 20–60 μm, 40–100 μm, 80–130 μm.
(c) Cellulose filter paper: High surface roughness, high distribution of pore sizes, non-transparent.
(d) Fried potato crusts: Very high surface roughness, high distribution of pore sizes, non-transparent.

Siloxane oils (Brookfield) with nominal viscosities of 5, 10, 50 and 100 mPa s were used as wicking liquids. The choice of siloxane oils for the present experiments is based on the following properties: (a) they are low energy liquids forming a precursor film during wetting, (b) they practically do not evaporate under the experimental conditions and (c) due to their viscosity they penetrate the above samples at low wicking rates; this prevents dynamic contact angle effects. More details on the above can be found in previous works [8,10,12]. Siloxane oils are transparent liquids, the same holds for many of the liquids used in wicking tests. This makes the detection of the wicking front much more difficult than in the case of a coloured wicking liquid. Nevertheless, the choice of transparent liquids was necessary in order to account for even the most difficult experimental cases.

The wicking experiments were performed by using the set-up presented in Fig. 3. A CCD camera (Sony, XC-73CE) part of an axisymmetric drop shape analysis instrument (CAM200, KSV) was used to acquire the images. This camera acquired greyscale images. In order to examine the capability of the program to analyse colour images some of the experiments were monitored using a digital colour camera (Legria HF R106, Canon). For all wicking experiments small parts of the material (approximately 10 mm × 10 mm) were examined at high resolution and magnification in order to be able to observe local heterogeneities within the material. The wicking experiments included experiments under optimal conditions (good contrast between wetted and non-wetted areas, uniform lighting) some experiments were also conducted under “difficult” for the analysis conditions. The “difficult” conditions included deliberately caused lighting disturbances (uneven lighting, shadows, lighting that changes over time, etc.), bad contrast, reflecting surfaces, material presenting uneven wicking front, materials presenting high

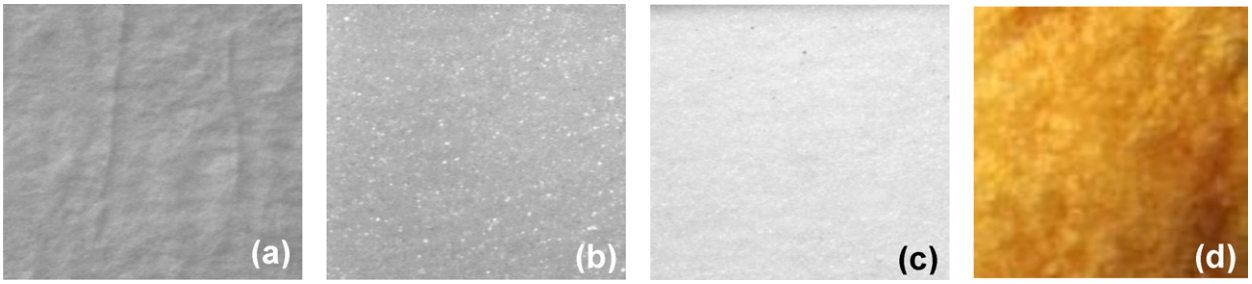

Fig. 2. Examples of material used for the wicking tests (a) cellulose filter paper, (b) glass porous medium and (c) polymer porous medium (d) fried potato crust (image actual width for (a)–(c) approx. 6 mm, for (d) approx. 3 mm).

surface roughness, etc. The "difficult" conditions aimed to best simulate actual experimental conditions and further stress the capabilities of the algorithm. On the whole more than 50 wicking experiments were conducted in order to examine the capabilities of our application.

All dynamic wicking data were analysed with the use of the developed program. The correct analysis of the program was verified by checking the position of the line drawn in the output images. Furthermore, for some characteristic cases the results of the program were compared to those analysed "manually". This was done by drawing a line on the position of the wicking front and the determining the distance in the images. For this reason Corel Draw 12 was used.

4. Results and discussion

Fig. 4 presents typical results obtained for a "normal" case ((a) and (b)) and two "difficult" cases ((c) to (f)). In the figure the measured squared height (h^2) as a function of time (t) (Fig. 4a, c and e) is presented. This representation of data was chosen because it is used as an input to the Washburn equation. Fig. 4b, d and f presents a few characteristic images given as an input to the program (upper line of each figure) and taken as an output (lower line of each figure). In the so-called "normal" case (Fig. 4b, images in the upper line) there is a good contrast between wetted and non wetted areas, the wicking front is even and there are no shadows or grey spots caused by the material roughness. The program is able to detect the wicking front and draw a straight line at its position (compare images in the upper line with those of the lower line in Fig. 4b). The h^2 vs t results are shown in Fig. 4a; results obtained by the program are compared with those obtained manually. Results obtained by the two methods almost coincide and as a consequence the slope of the lines describing the h^2 vs t data to be used as an input to the Washburn equation is the same.

Fig. 4c and d shows results on one of the difficult cases: the front is uneven but not exceedingly fluctuating to require local analysis. In addition, the contrast between wetted and non-wetted areas is worst than in the previous case and several grey spots appear in the image as a result of the surface roughness of the material. Finally, a horizontal shadow appears in the material. Again, comparing the input and output images of the program the definition of the wicking front position is satisfactory (Fig. 4d). Results on h^2 vs t obtained manually and by the software are similar. The slopes of the lines describing the data differ only slightly (1.9%). Such differences are not surprising if one takes into account that there is a 2.0% change in the slope if there is a difference in the determination of the size of reference scale of only 1 pixel which is our resolution of determining the reference scale size.

Fig. 4e and f presents another "difficult" case for the software: the material is light reflecting (this is why the intensity of light was decreased and resulted in darker images), the contrast is not good and the front is uneven. Again, the determination of the position of the wicking front is satisfactory (Fig. 4f) and results obtained by the programme are comparable to those obtained manually.

Fig. 5 presents results for a cellulose filter. As shown in the snapshot (Fig. 5b) a highly fluctuating wicking front was observed. For such wicking data one could follow the same analysis as the one followed in Fig. 4 and determine in this case average properties. However, for such highly fluctuating wicking front we consider it preferable to make a local analysis of the images. For this reason we divided the images into 4 areas. This was dictated by the number of areas in this particular experiment where differences in wicking velocities were observed (Fig. 5b). For another material the number of areas can be increased or decreased. As can be seen in Fig. 5a the material properties vary along the horizontal axis as depicted by the different positions of the wicking front determined at the different areas (different data series). In addition the material properties vary also along the vertical axis (differences in the slope of the h^2 vs t line in the same group if data). Measurements in the cellulose filter were repeated by using different pieces of the material. The results showed that the variations of wicking rates presented in Fig. 5 are more or less pronounced in different positions along the material. Therefore, in order to provide representative and statistically significant results measurements need to be repeated several times using different parts of the material. The above results may be significant for the cellulose filter performance which seems to vary slightly. Such a wicking test could be a quality control tool for the performance of such a filter. For example an increase in the wicking rate compared to what is customarily measured for a certain type of filter, would reflect higher filter pore sizes (wicking measurements with apolar liquids). This characteristic could be local or global. Such a result means that the filter allows a group of particles to pass through which normally should be retained by it.

Fig. 6 presents results on a fried potato crust (the crust was dry and deoiled before performing the wicking experiments). The fact that the liquid wicks the porous crust show that the pores of the crust are interconnected. In this case, there is no fluctuation of the wicking front but the central part of the crust presents at some

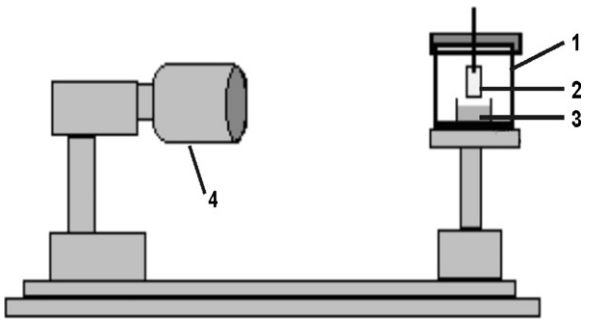

Fig. 3. Experimental set-up used for the wicking tests. (1) Optical glass cell, (2) porous medium, (3) wicking liquid and (4) CCD camera interfaced to a PC.

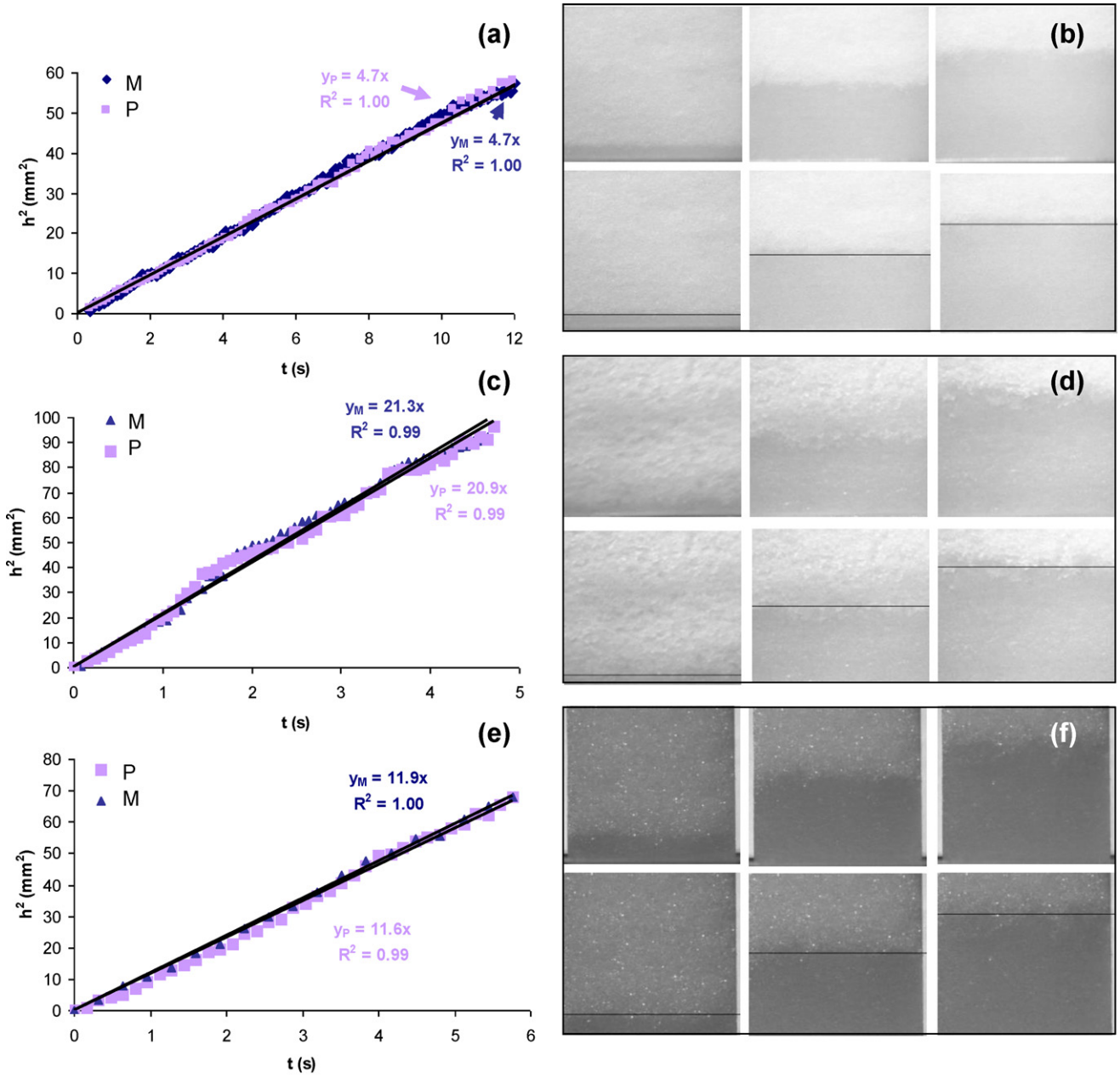

Fig. 4. Example results on a "normal" wicking case ((a) and (b)) and on two "difficult" cases ((c)–(f)). In (a), (c) and (e) results obtained by the program (P) are compared to those obtained manually (M). *h* is the wicking height and *t* the time. Figures (b), (d) and (f) show some characteristic input (upper line) and output (lower line) images of the program.

points a much faster wicking rate than the rest (Fig. 6a). For this reason it was decided to analyse the central part of the images and compare it with results obtained for the whole width of the crust. Analysis of the images shows that the wicking rate of the central part is overall faster than the wicking rate of the whole width of the material. Furthermore, the central part of the material presents changes in the wicking rate along its height. Such a characteristic should not be considered as typical of the central part of the crust because other potato crusts present high wicking rates in other positions (not shown). The differences in the wicking rates reflect differences in the potato crust pore sizes created by water removal in the form of bubbles during frying. According to the differences in wicking rates larger pores are more than an order of magnitude larger compared to the smaller ones. One might find such high differences in pore sizes surprising because the potato consists of cells of practically the same size. Yet, such high differences in pore sizes have been observed by scanning electron microscopy [13]. Oil uptake in French-fries occurs in the crust region extending 300–500 μm from the potato surface after the removal of potatoes from the fryer [14,15]. Due to the significant local differences in crust pore sizes oil uptake occurs much faster in the larger pores than in the smaller ones. These larger pores, which are first filled with oil, may act as oil reservoirs for oil penetration in the neighbour smaller ones which are filled with oil later on. This would suggest that oil penetration in French-fry crusts occurs in two dimensions (a) from the oil film on the potato surface towards the potato core crust-interface and (b) from the larger to the smaller neighbouring pores in parallel to the potato surface.

Both examined biological material presented a heterogeneous structure in terms of porous structure, heterogeneity in terms of surface properties was not considered due to the

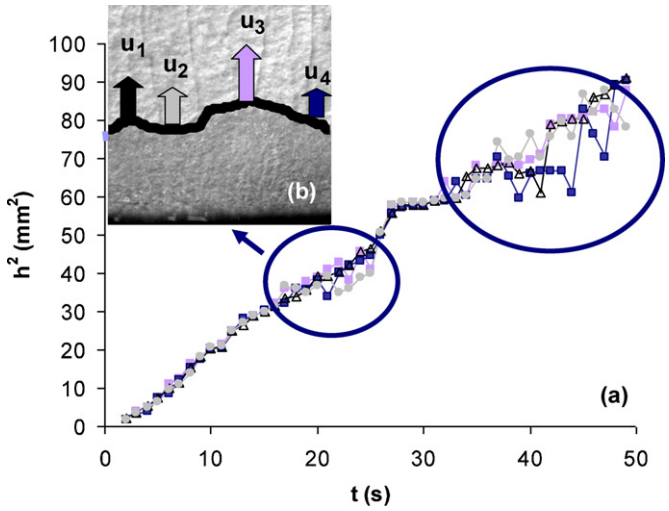

Fig. 5. Analysis of a wicking experiment presenting a fluctuation wicking front. In (a) the squared height (h^2) vs time (t) results are given for 4 different areas of the material presenting locally different wicking velocities (u_1–u_4) as shown in (b).

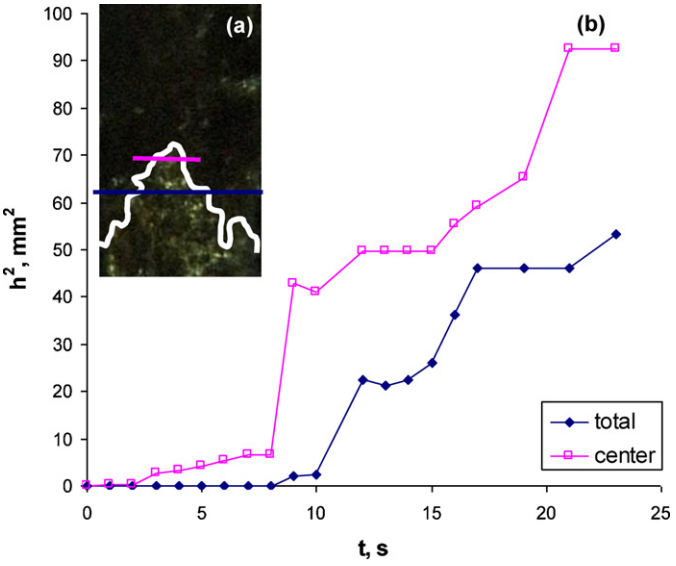

Fig. 6. Dynamic wicking results on a fried potato crust. In (a) a characteristic image with the two lines representing the output of the analysis for the central part (magenta) and whole width (blue) analysis. In (b) squared height (h^2) vs time (t) results of the wicking experiment. (For interpretation of the references to colour in this figure legend, the reader is referred to the web version of the article.)

chemical composition of the material. In the case of a material presenting a local variation in surface properties the wicking rate would vary locally when liquids of different surface tensions are used.

5. Conclusions

In this work an algorithm, program and software for the analysis of optical wicking data has been developed. The program can provide averaged information on the whole material as well as local information. The local analysis of the optical wicking data in a porous medium or powder can be a means to describe its heterogeneous nature in terms of pore sizes and/or surface properties. Such information has not been quantitatively exploited in the past. The application is simple and can be used as a tool of an axisymmetric drop shape analysis instrument or to analyse data from a stand-alone camera. In order to develop and test the program a big number of wicking experiments with different material and different lighting conditions has been performed. The program performed well under all examined conditions. Finally, the program was used in order to analyse two biological materials: a cellulose filter and a fried potato crust. Both material presented an uneven wicking front reflecting a variation in pore sizes and the optical wicking data were analysed locally. The results on the cellulose material could prove significant for its filtering performance. On the other hand analysis of the wicking data of the porous crust showed differences in pore sizes of approximately an order of magnitude and suggested that oil uptake does not occur simultaneously in the whole crust but first in the larger pores and then in the smaller ones.

Role of the funding source

The Research Committee of ATEI of Thessaloniki (funding source of the present work) had no involvement in study design; in the collection, analysis, and interpretation of data; in the writing of the report; and in the decision to submit the paper for publication.

Acknowledgements

This work was funded by the Research Committee of Alexander Technological Educational Institution of Thessaloniki. The aid of O. Stouraiti and E. Athanasiou in the wicking experiments is greatly acknowledged.

Appendix A.

Steps of the algorithm used to calculate the wicking front from a set of images

```
1       //FI, list of images
2       //FT, fill threshold which represents the sensitivity of the algorithm
3       calculate_distances(FI, FT)
4       YTOP = get_max_image_height(FI)
5       foreach F in FI do
6       YTOP, H = process_file(F, YTOP+8, FT)
7       R{}(get_file_name(F), H-YTOP)
8
9       //F, Image file
10      //START, previous value of the wicking front in pixels
11      process_file(F, START, FT)
12      IW, IH = get_image_dimensions(F)
13        I = I0 = load_image(F)
14      apply_blur_and_stretch_contrast(I)
15        I1 = copy(I)
16
17      if START >= IH then
18      YTOP = IH-10
19      else if START < 0 then
20      YTOP = IH + START
21      else
22      YTOP = START
23
24      while True do
25      Y2 = ((IH-YTOP-1)*0.3) + YTOP
26            YTOP2 = IH
27
28      foreach X in [0,10) do
29      XTOP2B, YTOP2B = process_section(I, I1, IW*X/10, Y2, FT)
30
31      if YTOP2B < YTOP then
32      XTOP2 = XTOP2B
33      YTOP2 = YTOP2B
34
35            If YTOP2 >= YTOP:
36              break
37
38      YTOP = YTOP2
39        return YTOP, IH
```

```
40
41 //IMGIN, Input image which represents the currently examined image
42 //IMGOUT, Output image containing the filled pixels
43 process_section(IMGIN, IMGOUT, X, Y, FT)
44 IW, IH = get_image_dimensions(F)
45 IMGDONE = create_image(IW, IH)
46 LISTOFPOINTS = {(X,Y)}
47    START_COLOR = get_pixel_color(IMGIN, X, Y)
48 XTOP = X
49 YTOP = Y
50
51 foreach P in LISTOFPOINTS do
52 X0, Y0 = P
53 P_COLOR = get_pixel_color(IMGIN, X0, Y0)
54
55 foreach DX in [-1, 1] do
56         foreach DY in [-1, 1] do
57            X=X0+DX
58            Y=Y0+DY
59            TOUT=get_pixel_color(IMGOUT, X, Y)
60            TDONE=get_pixel_color(IMGDONE, X, Y)
61
62            if X not in [0, IW] or Y not in [0, IH] or TOUT==0 or TDONE==0 then
63               continue
64
65            set_pixel_color(IMGDONE, X, Y, 0)
66            COLOR = get_pixel_color(IMGIN, X, Y)
67
68            if COLOR < START_COLOR+2*FT and COLOR < P_COLOR+FT then
69 set_pixel_color(IMGOUT, X, Y, 0)
70 LISTOFPOINTS{}(X,Y)
71
72            if Y<YTOP then
73               XTOP = X
74               YTOP = Y
75   return XTOP, YTOP
```

References

[1] C.J. van Oss, R.F. Giese, Z. Li, K. Murphy, J. Norris, M.K. Chaudhury, R.J. Good, Determination of contact angles and pore sizes of porous media by column and thin layer wicking, J. Adhes. Sci. Technol. 6 (1992) 413–428.

[2] E. Chibowski, L. Holysz, Use of the Washburn equation for surface fee energy determination, Langmuir 8 (1992) 710–716.

[3] E.P. Kalogianni, T. Savopoulos, T.D. Karapantsios, S.N. Raphaelides, A dynamic wicking technique for determining the effective pore radius of pregelatinized starch sheets, Colloids Surf. B 35 (2004) 159–167.

[4] J. Navas, R. Alcántara, C. Fernández-Lorenzo, J. Martín-Calleja, Pore characterization methodology by means of capillary sorption tests, Transp. Porous Med. 86 (2011) 333–351.

[5] E.W. Washburn, The dynamics of capillary flow, Phys. Rev. 17 (1921) 273.

[6] R. Morent, N. De Geyter, C. Leys, E. Vansteenkiste, J. De Bock, W. Philips, Measuring the wicking behaviour of textiles by the combination of a horizontal wicking experiment and image processing, Rev. Sci. Instrum. 77 (2006) 093502.

[7] M. Conrath, N. Fries, M. Zhang, M.E. Dreyer, Radial capillary transport from an infinite reservoir, Transp. Porous Med. 84 (2010) 109–132.

[8] A. Marmur, R.D. Cohen, Characterization of porous media by the kinetics of liquid penetration: the vertical capillaries model, J. Colloids Interface Sci. 189 (1997) 299.

[9] L. Labajos-Broncano, M.L. González-Martín, J.M. Bruque, On the evaluation of the surface free energy of porous and powdered solids from imbibition experiments: equivalence between height–time and weight–time techniques, J. Colloids Interface Sci. 262 (2003) 171–178.

[10] E.P. Kalogianni, Physico-chemical and chemical changes during deep-frying of potatoes, Ph.D. Thesis, Lincoln University, Lincoln, UK, 2007.

[11] C.J. Budziak, A.W. Neumann, Automation of the capillary rise technique for measuring contact angles, Colloids Surf. 43 (1990) 279–293.

[12] J. Daillant, J.J. Benattar, L. Leger, Ultrathin film in wetting evidenced by X-ray reflectivity, Phys. Rev. A: Atom. Mol. Opt. Phys. 41 (1990) 1963–1977.

[13] G. Lisińska, G. Gołubowska, Structural changes of potato tissue during French-fries production, Food Chem. 93 (2005) 681–687.

[14] G. Ufheil, F. Escher, Dynamics of oil uptake during deep-fat frying of potato slices, Lebensm. Wiss. Technol. 29 (1996) 640–644.

[15] R.G. Moreira, X. Sun, Y. Chen, Factors affecting oil uptake in tortilla chips in deep-fat frying, J. Food Eng. 31 (1997) 485–498.